Article

Cell Reports

The Nav1.9 Channel Is a Key Determinant of Cold Pain Sensation and Cold Allodynia

Graphical Abstract

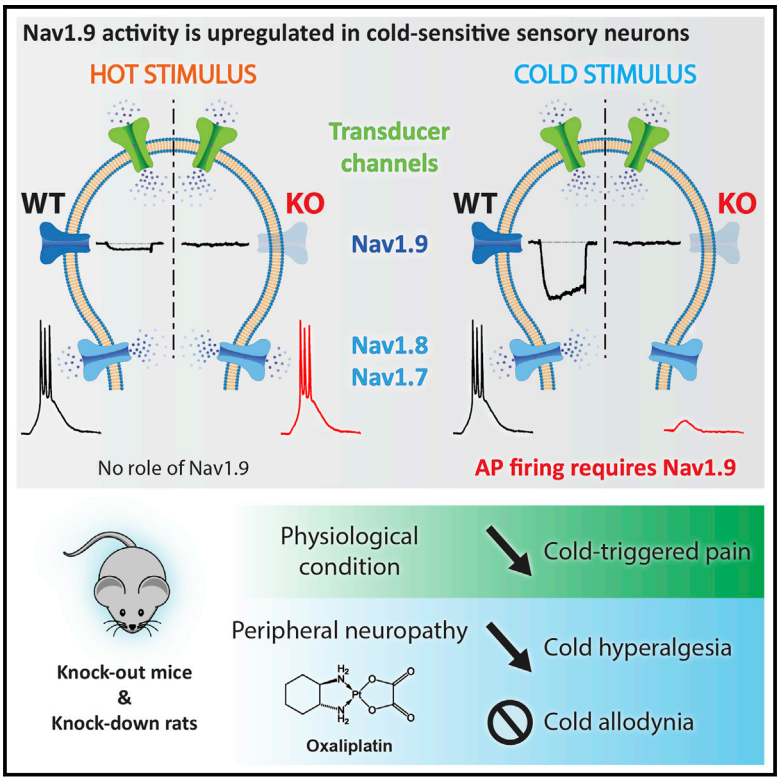

Highlights

- Nav1.9 acts as a subthreshold amplifier in cold-sensitive sensory neurons
- Action potential firing in response to cold exposure requires functional Nav1.9
- Cold-triggered pain is reduced in mice and rats deficient for Nav1.9
- Oxaliplatin-induced cold allodynia is absent in animals deficient for Nav1.9

Authors

Stéphane Lolignier, Caroline Bonnet, ..., Patrick Delmas, Jérôme Busserolles

Correspondence

patrick.delmas@univ-amu.fr (P.D.), jerome.busserolles@udamail.fr (J.B.)

In Brief

Lolignier et al. show that Nav1.9 is important for the perception of cold-triggered pain. Nav1.9 current is upregulated in cold-sensitive sensory neurons, where it acts as a subthreshold amplifier, allowing firing upon exposure to noxious cold. Painful cold hypersensitivity following oxaliplatin chemotherapy is also reduced in rodents deficient for Nav1.9.

Lolignier et al., 2015, Cell Reports *11*, 1067–1078
May 19, 2015
http://dx.doi.org/10.1016/j.celrep.2015.04.027

CellPress

Cell Reports
Article

The Nav1.9 Channel Is a Key Determinant of Cold Pain Sensation and Cold Allodynia

Stéphane Lolignier,[1,2] Caroline Bonnet,[3] Christelle Gaudioso,[3] Jacques Noël,[5] Jérôme Ruel,[3] Muriel Amsalem,[3] Jérémy Ferrier,[1,2] Lise Rodat-Despoix,[3] Valentine Bouvier,[3] Youssef Aissouni,[1,2] Laetitia Prival,[1,2] Eric Chapuy,[1,2] Françoise Padilla,[3] Alain Eschalier,[1,2,4] Patrick Delmas,[3,6,*] and Jérôme Busserolles[1,2,6,*]
[1]Pharmacologie Fondamentale et Clinique de la Douleur, Clermont Université, Université d'Auvergne, 63000 Clermont-Ferrand, France
[2]Inserm, U 1107, Neuro-Dol, 63000 Clermont-Ferrand, France
[3]Aix-Marseille-Université, CNRS, Centre de Recherche en Neurobiologie et Neurophysiologie de Marseille, UMR 7286, CS80011, Bd Pierre Dramard, 13344 Marseille Cedex 15, France
[4]Service de Pharmacologie, CHU Clermont-Ferrand, 63003 Clermont-Ferrand, France
[5]Institut de Pharmacologie Moléculaire et Cellulaire, LabEx ICST, UMR 7275 CNRS, Université de Nice Sophia Antipolis, 06560 Valbonne, France
[6]Co-senior author
*Correspondence: patrick.delmas@univ-amu.fr (P.D.), jerome.busserolles@udamail.fr (J.B.)
http://dx.doi.org/10.1016/j.celrep.2015.04.027

SUMMARY

Cold-triggered pain is essential to avoid prolonged exposure to harmfully low temperatures. However, the molecular basis of noxious cold sensing in mammals is still not completely understood. Here, we show that the voltage-gated Nav1.9 sodium channel is important for the perception of pain in response to noxious cold. Nav1.9 activity is upregulated in a subpopulation of damage-sensing sensory neurons responding to cooling, which allows the channel to amplify subthreshold depolarizations generated by the activation of cold transducers. Consequently, cold-triggered firing is impaired in *Nav1.9*$^{-/-}$ neurons, and *Nav1.9* null mice and knockdown rats show increased cold pain thresholds. Disrupting *Nav1.9* expression in rodents also alleviates cold pain hypersensitivity induced by the antineoplastic agent oxaliplatin. We conclude that Nav1.9 acts as a subthreshold amplifier in cold-sensitive nociceptive neurons and is required for the perception of cold pain under normal and pathological conditions.

INTRODUCTION

The ability to detect high-intensity and potentially harmful physicochemical stimuli is a vital function conserved among the animal kingdom. In mammals, pain is triggered by the activation of a subclass of high-threshold sensory neurons called nociceptors, which are dedicated to the detection of a wide variety of noxious stimuli.

The molecular basis of nociceptor activation by extreme temperatures remains incompletely understood, particularly when considering cold nociception. Searches for ion channels responding to cold led to the cloning of TRPM8 (McKemy et al., 2002; Peier et al., 2002). This cation channel is directly activated by innocuous cooling (<28°C) and in vivo studies showed an involvement of TRPM8 channels in thermal discrimination below 25°C (Bautista et al., 2007; Dhaka et al., 2007). More recent studies have also shown a role for TRPM8 channels and *TRPM8*-expressing neurons in cold-triggered nociception (Pogorzala et al., 2013; Knowlton et al., 2013). Although TRPM8 involvement in non-noxious thermal discrimination below 25°C is undisputable, its involvement in cold-triggered nociception remains unclear. Another thermo-TRP channel, namely TRPA1, was later reported to be activated by noxious cold in vitro (Story et al., 2003). However, its function as a sensor for noxious cold in vivo is still debated (Bautista et al., 2006; Gentry et al., 2010; Kwan et al., 2006), and the human TRPA1 isoform has been shown to be either cold insensitive (Chen et al., 2013) or cold sensitive (Moparthi et al., 2014). In addition, a third of the cold-responding sensory neurons in dorsal root ganglia (DRGs) expresses neither *TRPM8* nor *TRPA1* (Munns et al., 2007), indicating that a subset of sensory neurons relies on a different channel to transduce cold. The TRPC5 channel was also reported to be cold sensitive, and experiments carried out on knockout mice indicated that this channel contributes to cold discrimination in the non-noxious range (Zimmermann et al., 2011). Finally, two-pore-domain potassium channels were found to play a key role in cold transduction. Genetic ablation of *TREK-2* or *TREK-1* and *TRAAK* channels together shifts the activation threshold of sensory neurons, and the pain threshold of animals, to less extreme cold temperatures (Noël et al., 2009; Pereira et al., 2014). The TASK-3 channel was also recently shown to be important for the transduction of cold in TRPM8-positive neurons (Morenilla-Palao et al., 2014). In spite of these advances, a clear picture of the molecular events contributing to the transduction of noxious cold has yet to emerge, and more work is needed to identify the proteins involved in cold nociception.

A better understanding of the molecular basis of cold pain sensation could have a significant clinical impact. Indeed, neuropathic conditions are remarkably associated with cold-triggered

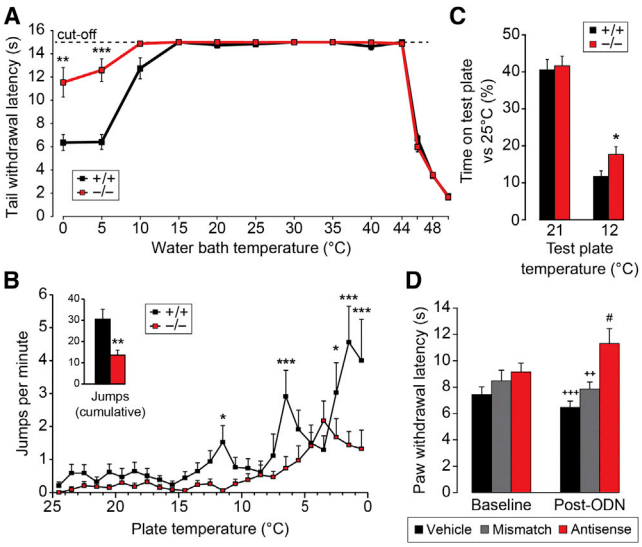

Figure 1. Nav1.9 Is Required for Normal Cold Nociception in Rodents

(A) Thermal pain thresholds of *Nav1.9*$^{-/-}$ mice and WT littermates, evaluated with the tail immersion test at temperatures from 0°C to 50°C. n = 24 +/+, n = 16 −/−.

(B) Jumps produced by WT and *Nav1.9*$^{-/-}$ mice on a plate cooled from 25°C to 0°C at a 1°C • min^{-1} rate. n = 34.

(C) Percentage of time spent on the test plate (21°C or 12°C) versus the control plate (set at 25°C) by WT and *Nav1.9*$^{-/-}$ mice over a 3-min thermal preference test. n = 26.

(D) Thermal pain threshold of rats submitted to the 5°C paw immersion test before and after *Nav1.9* knockdown. n = 8. *p < 0.05, **p < 0.01, ***p < 0.001 versus +/+; $^{\#}$p < 0.05 versus baseline; $^{++}$p < 0.01, $^{+++}$p < 0.001 versus antisense; Mann and Whitney rank sum test (A, inset in B), two-way ANOVA followed by Student-Newman-Keuls' test (B and D), unpaired t test (C). Error bars correspond to SEM.

pain or cold hypersensitivity in humans, with the most dramatic example being brought by oxaliplatin-based chemotherapy. This neurotoxic compound induces a peripheral neuropathy characterized by debilitating cold hypersensitivity and cold-triggered pain or paresthesia in up to 90% of treated patients (Kiernan, 2007), and the molecular mechanisms underlying this painful state remain largely elusive.

Because sensory discrimination can be reflected by the ability of sensory neurons to generate action potentials at innocuous and noxious cold temperatures, we focused our interest on voltage-gated sodium channels. It has previously been shown that cooling facilitates firing in sensory neurons displaying tetrodotoxin-resistant (TTX-R) sodium currents, whereas it suppresses firing in tetrodotoxin-sensitive (TTX-S) neurons (Sarria et al., 2012). Moreover, the TTX-R sodium channel Nav1.8 (Fukuoka et al., 2008) is essential for nociceptors activity at low temperatures and for the reaction of mice in response to noxious cold (Zimmermann et al., 2007). In this context, we found that the TTX-R voltage-gated sodium channel Nav1.9 (Baker et al., 2003; Coste et al., 2004; Cummins et al., 1999; Herzog et al., 2001; Padilla et al., 2007), known to date for being involved in inflammatory and, to some extent, neuropathic pain (Amaya et al., 2006; Leo et al., 2010; Lolignier et al., 2011; Priest et al., 2005), is required for cold nociception. Nav1.9 channels remain functional at low temperatures and exhibit enhanced activity in a subset of sensory neurons responding to cold. Consistently, activation of *Nav1.9*$^{-/-}$ nociceptors by cold is reduced, making these neurons unable to reach firing threshold in response to cooling. Disrupting *Nav1.9* expression impairs behavioral responses to noxious cold stimuli in mice and rats. In addition, oxaliplatin-induced cold hypersensitivity is reduced in *Nav1.9* knockout mice and knockdown rats. Collectively, these findings demonstrate that Nav1.9 is important for the integration of cold stimuli in both physiological and pathological conditions.

RESULTS

Nav1.9 Is Necessary for Cold-Triggered Nociception In Vivo

The contribution of Nav1.9 to thermal nociception was first examined by submitting WT and *Nav1.9*$^{-/-}$ mice to the tail immersion test. While the pain threshold of *Nav1.9*$^{-/-}$ mice in response to heat was unchanged when compared with WT littermates, these animals showed a 2-fold increase in reaction thresholds to noxious cold (0°C and 5°C; Figure 1A). This observation was unexpected as the Nav1.9 channel has been shown to be not involved in the flinching behavior of mice placed on a 0°C cold plate (Amaya et al., 2006). Another previous study suggests, however, that the early behaviors produced by mice on a cold plate, such as paw rubbing or shivering, are characteristic of thermal discrimination rather than cold-triggered nociception, the latter being observable through the jumping/escaping behavior induced by prolonged cold exposure (Karashima et al., 2009). To address this question, we submitted *Nav1.9*$^{-/-}$ mice to both tests. In accordance with the previous study involving *Nav1.9*$^{-/-}$ mice, we observed no difference between the latency to flinches or paw rubbing of WT and *Nav1.9*$^{-/-}$ mice placed on a 0°C or 6°C cold plate, or in the number of flinches produced by mice placed on a 0°C plate for 5 min (Figure S1). However, we observed a significant reduction in the number of jumps produced by *Nav1.9*$^{-/-}$ mice subjected to a cold ramp test on a plate decreasing from 25°C to 0°C at a 1°C • min^{-1} rate for temperatures of 12°C and below (Figure 1B), showing the role played by Nav1.9 in cold nociception. We further validated these observations by submitting *Nav1.9*$^{-/-}$ mice to the thermal preference test (Figure 1C). Both WT and *Nav1.9*$^{-/-}$ mice showed a preference for the warmest plate when the choice was given between 25°C and 12°C or between 25°C and 21°C, showing that *Nav1.9* deletion does not impair thermal discrimination. However, *Nav1.9*$^{-/-}$ mice showed less avoidance for the 12°C plate than the WTs, confirming the involvement of the channel in cold nociception from 12°C. The number of transitions between the two plates was unaffected, showing similar motor activity, and no preference for a plate was found when they were both set at 25°C (Figure S2). Motor deficit in *Nav1.9*$^{-/-}$ mice was not observed neither in previous studies involving extensive evaluation of motor activity and motor coordination (Amaya et al., 2006; Priest et al., 2005).

To rule out the possibility of a bias caused by compensatory mechanisms in the knockout and to extend our observations to another rodent model, we assessed the cold-pain threshold of rats following *Nav1.9* knockdown by intrathecal injection of

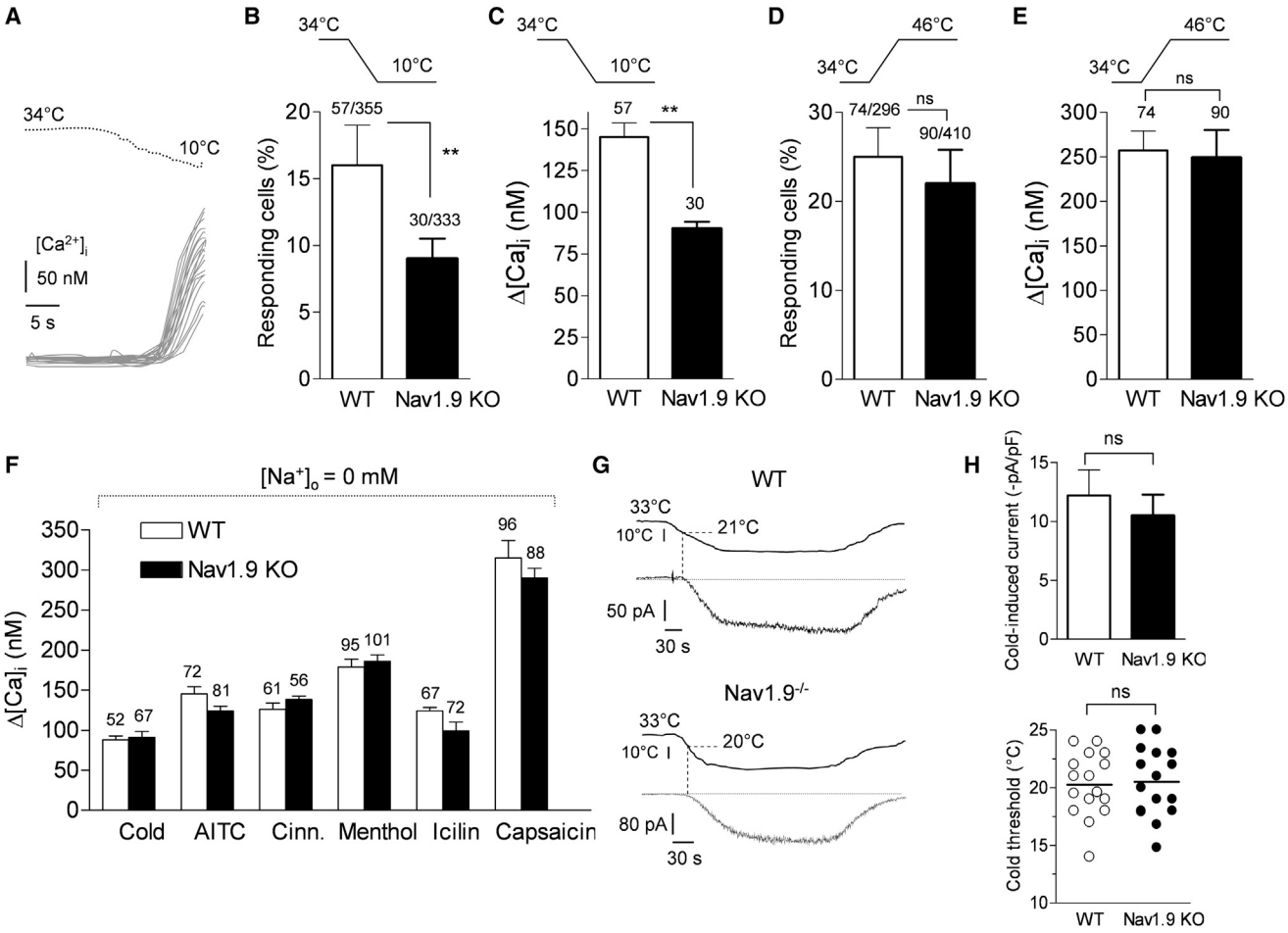

Figure 2. Response to Cooling Is Impaired in *Nav1.9*$^{-/-}$ DRG Neurons

(A) Representative examples of calcium responses induced by a cooling ramp (upper trace) in cold-sensitive WT DRG neurons.

(B and C) Histograms show the percentage of WT and *Nav1.9*$^{-/-}$ neurons responding to a cooling ramp (B) and the mean $\Delta[Ca^{2+}]_i$ amplitude of the response (C). The number of cells is indicated above the error bars.

(D and E) Percentage of WT and *Nav1.9*$^{-/-}$ neurons responding to a heating ramp (D) and mean $\Delta[Ca^{2+}]_i$ amplitude (E).

(F) $\Delta[Ca^{2+}]_i$ response induced by cold (ramp from 34°C to 10°C) or by the chemical agonists of TRPA1 (50 μM AITC, 100 μM cinnamaldehyde), TRPM8 (250 μM menthol, 50 μM icilin), and TRPV1 (1 μM capsaicin) in WT and *Nav1.9*$^{-/-}$ neurons using sodium-free extracellular solution to suppress the contribution of sodium channels to neuronal activation.

(G) Representative inward currents generated by cooling in WT and *Nav1.9*$^{-/-}$ neurons held at −60 mV. KCl-based pipette solution.

(H) Amplitude of the cold-induced current (upper) and its apparent threshold (lower) determined in WT and *Nav1.9*$^{-/-}$ DRG neurons. Horizontal bars represent mean values. **$p < 0.01$; ns, not significant; unpaired t test. Error bars correspond to SEM.

antisense oligodeoxynucleotides (ODNs), as we previously described (Lolignier et al., 2011). Nav1.9 expression in DRGs was reduced by 70% in antisense-treated animals compared with those that received injections of saline or scramble mismatch ODNs (Figure S3). We observed an increased pain threshold to 5°C paw immersion in rats treated with *Nav1.9* antisenses, while saline or mismatch ODNs had no effect (Figure 1D). Altogether, these results demonstrate the involvement of Nav1.9 in cold nociception in mice and rats.

Nav1.9 Is Involved in Setting the Sensory Neuron Response to Cold

Sensory neurons cultured from WT and *Nav1.9*$^{-/-}$ mouse DRGs were assessed for functional cold sensitivity with cooling ramps from 34°C to 10°C while following neuronal activation using ratiometric calcium imaging. A strong reduction in the proportion of cold-sensitive neurons was observed in *Nav1.9*$^{-/-}$ compared with WT cultures (Figures 2A and 2B). In addition, *Nav1.9*$^{-/-}$ neurons that responded to cold did so with a reduced increase in calcium levels (Figure 2C). In contrast, the percentage of neurons responding to a heating ramp (34°C to 46°C) was unchanged in cultures from *Nav1.9*$^{-/-}$ DRGs (Figure 2D), and the increase in calcium levels induced by heat was likewise unaltered (Figure 2E). We then used sodium-free extracellular solution to suppress the contribution of Na^+ channels to neuronal activation and isolate the response mediated by cold-sensitive transducer channels (Figure 2F). Under these conditions, cold-induced intracellular calcium increase was undistinguishable between

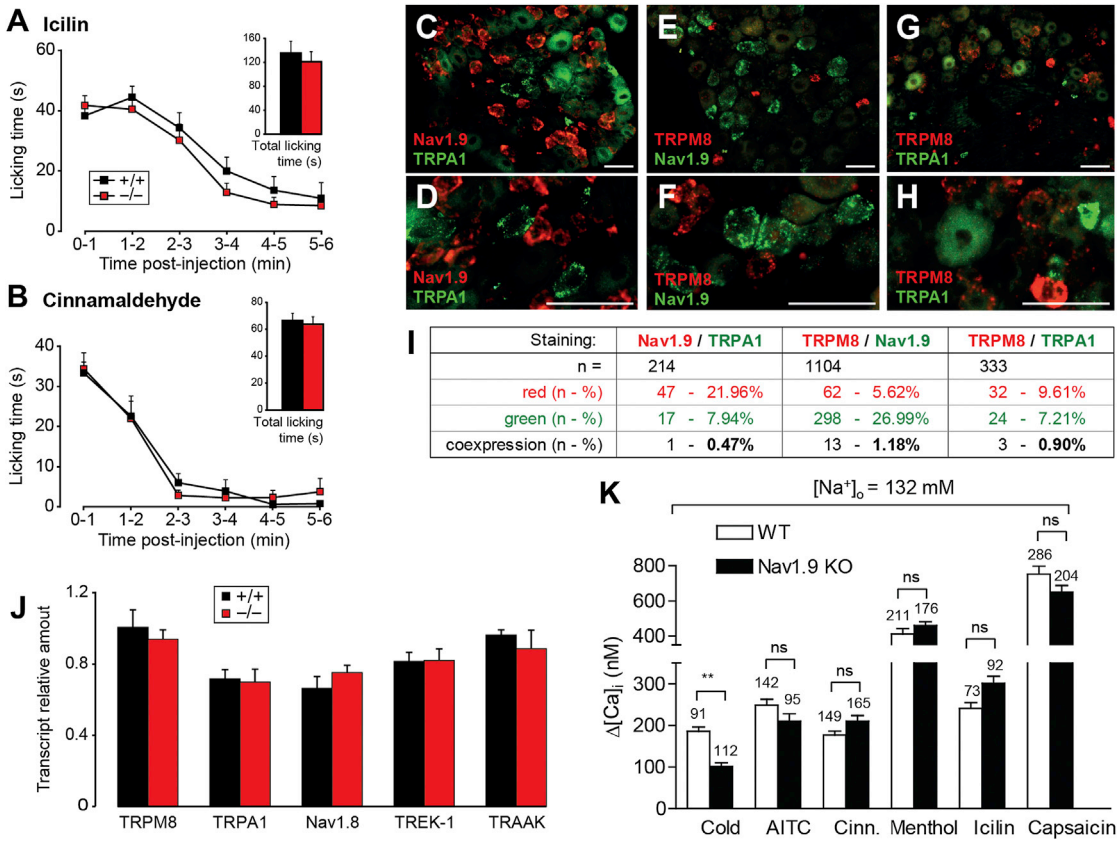

Figure 3. The Response to TRPM8 and TRPA1 Agonists and the Expression of Cold Pain-Related Genes Are Unchanged in *Nav1.9*$^{-/-}$ Mice Compared with WTs

(A and B) Nociceptive behavior (paw licking) subsequent to peripheral TRPM8 (A) and TRPA1 (B) activation by subplantar injection of their respective agonists icilin and cinnamaldehyde (both at 14 mM, 25 μl) in WT and *Nav1.9*$^{-/-}$ mice. n = 10.

(C–I) Co-staining of Nav1.9 and TRPA1 (C and D), Nav1.9 and TRPM8 (E and F), and TRPM8 and TRPA1 (G and H) by in situ hybridization in mice lumbar DRGs. Low magnifications (C, E, and G) and high magnifications (D, F, and H) are shown. Scale bars represent 50 μm. Quantification results are shown in (I), as raw cell numbers and percentages of neurons expressing either one transcript or both.

(J) Transcription level of putative cold transducers evaluated by qPCR in WT and *Nav1.9*$^{-/-}$ lumbar DRGs. n = 8.

(K) $\Delta[Ca^{2+}]_i$ response induced by a cold ramp from 34 to 10°C, 50 μM AITC, 100 μM cinnamaldehyde, 250 μM menthol, 50 μM icilin, or 1 μM capsaicin in WT and *Nav1.9*$^{-/-}$ neurons in presence of 132 mM extracellular sodium. **p < 0.01; unpaired t test (A and B, total licking time, J, K), two-way ANOVA (A and B, time course). Error bars correspond to SEM.

WT and *Nav1.9*$^{-/-}$ neurons. In addition, no difference in Ca^{2+} signal amplitude was seen between WT and *Nav1.9*$^{-/-}$ neurons in response to the chemical agonists of TRPA1 (allyl isothiocyanate [AITC], cinnamaldehyde), TRPM8 (menthol, icilin), and the heat-sensor TRPV1 (capsaicin).

We then examined the properties of cold-sensitive transducer currents in *Nav1.9*$^{-/-}$ and WT neurons of similar size (24–37 pF) using patch clamp recording (Figure 2G). Cooling from 33°C to 10°C generated a slowly activating inward current of −12.4 ± 2.0 pA/pF in 15% (n = 16/106) of the WT sensory neurons tested. This cold-induced current had a similar amplitude (−10.5 ± 1.9 pA/pF) in *Nav1.9*$^{-/-}$ neurons responding to the cooling ramp (n = 15/85, 17.6%; Figure 2H). The apparent activation temperature of this current was 20.3°C ± 0.4°C and 20.6°C ± 0.5°C in WT and *Nav1.9*$^{-/-}$ neurons, respectively (Figure 2H). These data show that the thermal transduction machinery is functional in *Nav1.9*$^{-/-}$ sensory neurons.

Nav1.9 Involvement in Cold-Induced Nociception Is Mostly Independent of the Thermo-TRP Channels TRPM8 and TRPA1

Nav1.9 has been proposed to act like a subthreshold amplifier, facilitating the reaching of the firing threshold by receptor potential, especially during inflammation when Nav1.9 current is upregulated (Herzog et al., 2001; Maingret et al., 2008; Hao et al., 2015). Nav1.9 knockout could therefore impair noxious cold sensitivity through raising the activation threshold of sensory neurons expressing TRPM8 or TRPA1.

To test this assumption, we activated TRPM8 and TRPA1 in sensory fibers in vivo by subplantar injection of their respective agonists icilin and cinnamaldehyde. Both drugs induced a nociceptive behavior characterized by acute licking of the injected paw. No difference in paw licking duration was observed between WT and *Nav1.9*$^{-/-}$ mice (Figures 3A and 3B), indicating

that Nav1.9 deletion does not disrupt inputs from TRPM8- or TRPA1-expressing sensory fibers.

We further examined whether Nav1.9 co-localizes with TRPM8 or TRPA1 in DRGs by in situ hybridization. As previously shown (Kobayashi et al., 2005), TRPM8 and TRPA1 were found to be primarily expressed in different subsets of sensory neurons (Figures 3G and 3H) as 3/24 (12.50%) TRPA1-positive neurons were also expressing TRPM8 and 3/32 (9.38%) TRPM8-positive neurons were also expressing TRPA1 (Figure 3I). Importantly, Nav1.9 co-localized poorly with TRPA1 (Figures 3C and 3D) or TRPM8 (Figures 3E and 3F), as Nav1.9 signal was found in only 1/17 TRPA1-positive neurons (5.88%) and 13/62 TRPM8-positive neurons (20.97%; Figure 3I). This suggests that Nav1.9 is involved in the cold response of a subclass of sensory neurons mostly devoid of TRPM8 and TRPA1.

Expression of putative cold-sensitive channels in WT and *Nav1.9*$^{-/-}$ mouse DRGs was also examined by real-time PCR. TRPM8, TRPA1, Nav1.8, TREK-1, and TRAAK channels were expressed at similar levels in DRGs from WT and *Nav1.9*$^{-/-}$ mice (Figure 3J). Finally, the increase in intracellular calcium levels induced by agonists of TRPA1 (AITC, cinnamaldehyde), TRPM8 (methol, icilin), or the heat sensor TRPV1 (capsaicin) were not different between WT and *Nav1.9*$^{-/-}$ sensory neurons when standard extracellular sodium concentration (132 mM) was used (Figure 3K). Under these conditions, we only observed a decrease in calcium response amplitude in *Nav1.9*$^{-/-}$ neurons challenged with a cooling ramp (from 34°C to 10°C).

Nav1.9 Current Is Functionally Upregulated in Cold-Sensitive Neurons

We next studied the impact of cooling on the Nav1.9 current isolated by adding TTX and Ca^{2+} channel blockers to the bath solution (Coste et al., 2007). We first recorded Na^+ current using a CsF-containing patch pipette solution, which helps to reveal the Nav1.9 current in DRG neurons (Coste et al., 2004). Cooling from 24°C to 10°C caused a slowing of activation and inactivation kinetics and reduced the peak current amplitudes of both Nav1.8 and Nav1.9 currents recorded in *Nav1.9*$^{-/-}$ and *Nav1.8*$^{-/-}$ sensory neurons, respectively (Figures 4A and 4B). On average, cooling inhibited Nav1.8 and Nav1.9 peak currents by 20% and 39%, respectively (Figure 4B), whereas inhibition reached 74% for TTX-S Na^+ current recorded in small DRG neurons (Figure S4). Nav1.9 current inhibition by cooling showed little dependence on the voltage, suggesting that cooling has little impact on the voltage-dependence of activation, as observed with Nav1.8 (Zimmermann et al., 2007).

We next sought to characterize the properties of the Nav1.9 current in sensory neurons responding to cold versus heat (Figure 4C). Nav1.9 current was recorded using a CsCl-based pipette solution to avoid alteration of its voltage dependence by internal fluoride (Coste et al., 2004; Maingret et al., 2008; Maruyama et al., 2004). To circumvent contamination arising from Nav1.8 currents, these experiments were performed in *Nav1.8*$^{-/-}$ sensory neurons. Cold and heat responding neurons were defined as neurons developing inward currents at −60 mV in response to cold or hot stimuli. Nav1.9 was detected in 47% of cold-sensitive *Nav1.8*$^{-/-}$ neurons and 66% of heat-sensitive *Nav1.8*$^{-/-}$ neurons. However, Nav1.9 current had a large amplitude (−82 pA/pF) in cold-sensitive neurons 8 min after achieving whole-cell mode, whereas it had a small amplitude (−4 pA/pF) in heat-sensitive neurons studied isochronally (Figures 4C–4E). Adding fluoride to the patch pipette solution modestly increased Nav1.9 current in cold-sensitive neurons, whereas it revealed a large Nav1.9 current in heat-sensitive neurons (Figures 4D and 4E). Similar results were obtained in cold-sensitive and heat-sensitive sensory neurons from WT DRGs (Figure 4E). Collectively, these data suggest that Nav1.9 channels are functionally upregulated in cold-sensitive neurons, whereas they show little constitutive activity in heat-sensitive neurons.

Nav1.9 Increases the Ability of Cold-Sensitive Neurons to Sustain Spiking upon Cooling

To determine to what extent Nav1.9 functional upregulation impacts on the excitability of cold-sensitive DRG neurons, we studied the excitability of WT and *Nav1.9*$^{-/-}$ nociceptors (18–35 pF) in response to a cooling ramp from 33°C to 10°C. Current clamp recordings were carried out with KCl-based pipette solution in steadily hyperpolarized neurons (∼−80 mV) in order to remove the slow inactivation of Nav1.9 channels (Coste et al., 2004; Cummins et al., 1999; Maingret et al., 2008). Figure 5A shows representative responses to cooling for both genotypes. We observed large cold-induced subthreshold depolarizations and bursts of action potentials in WT neurons. The responses showed signs of regenerative origin, typical of Nav1.9 (Coste et al., 2004; Maingret et al., 2008), adding to the cold-induced depolarizing response. In contrast, cold responses in *Nav1.9*$^{-/-}$ neurons lacked subthreshold amplification (Figure 5A). When left at resting potential while applying the cooling ramp (Figure 5B), WT neurons responded to the cold stimulation with sustained action potential discharges averaging ten spikes per stimulus (n = 19/114), whereas the cooling ramp failed to evoke sustained firing in many *Nav1.9*$^{-/-}$ neurons (n = 20/147), although these neurons kept their ability to fire action potentials in response to current injection (Figure 5B). On average, *Nav1.9*$^{-/-}$ neurons showed a 5-fold lower firing rate during the cooling ramp compared to WT neurons (Figure 5C). No alteration in heat-mediated firing discharges was seen in *Nav1.9*$^{-/-}$ heat-sensitive nociceptors (Figure 5D). These results indicate that the Nav1.9 current, in a subset of cold-sensitive nociceptors, produces subthreshold regenerative responses that amplify the cold transducer depolarization and facilitate spiking at low temperatures.

We finally performed skin-nerve preparations to characterize the contribution of Nav1.9 in the response to cold of sensory fibers in a more physiologically relevant context (Figures 5E–5H). Groups of fibers from the saphenous nerve were recorded while the temperature of a patch of skin was reduced from 30°C to 9°C–10°C. This resulted in an increase in spike frequency that was significantly diminished in *Nav1.9*$^{-/-}$ mice compared with WT. In *Nav1.9*$^{-/-}$ mice, we submitted the skin patch to a second cooling ramp subsequent to TRPM8 and TRPA1 blockade with BCTC and HC-030031; this caused a reduction in the cold-induced firing compared to untreated *Nav1.9*$^{-/-}$ fibers (Figures 5E, 5G, and 5H).

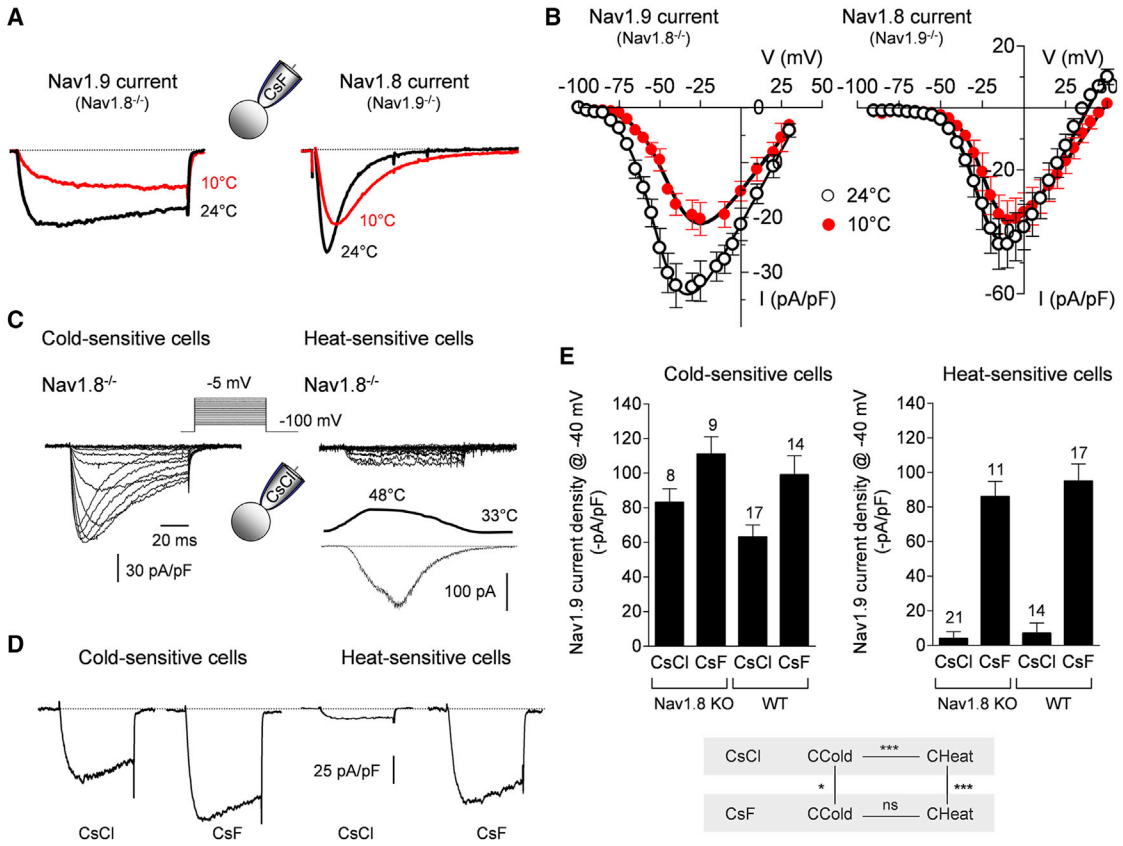

Figure 4. Nav1.9 Is Cold Resistant and Shows Enhanced Activity in Cold-Sensitive DRG Neurons

(A) Nav1.9 and Nav1.8 currents recorded in *Nav1.8*$^{-/-}$ and *Nav1.9*$^{-/-}$ neurons, respectively, were subjected to cooling from 24°C to 10°C. Nav1.9 current was evoked at −40 mV, whereas Nav1.8 was evoked at −10 mV. CsF-containing pipette solution was used.

(B) *I*(*V*) relationships for Nav1.9 (n = 9) and Nav1.8 (n = 11) determined at either 24°C or 10°C. Recording conditions are as in (A).

(C) Shown are representative Nav1.9 current traces recorded in a *Nav1.8*$^{-/-}$ DRG neuron responding to cooling (left) and in a neuron responding to heating (from 33°C to 48°C, right). CsCl-containing pipette solution.

(D) Nav1.9 currents recorded in cold- and heat-sensitive *Nav1.8*$^{-/-}$ DRG neurons using CsCl- and CsF-containing pipette solutions. Currents were evoked at −40 mV from a V_h of −100 mV.

(E) Nav1.9 current density (normalized to the cell membrane capacitance) recorded using either CsCl or CsF pipette solutions in cold-sensitive and heat-sensitive neurons. Currents were measured at −40 mV from a V_h of −100 mV. (Bottom) Statistical analysis comparing the amplitude of Nav1.9 currents recorded in heat- or cold-sensitive *Nav1.8*$^{-/-}$ neurons using the indicated recording conditions. *p < 0.05, ***p < 0.001; ns, not significant; unpaired t tests. Error bars correspond to SEM.

Oxaliplatin-Induced Cold Hypersensitivity Is Alleviated by Nav1.9 Knockout and Knockdown

Oxaliplatin is an antineoplastic agent widely used for the treatment of colorectal cancer. Its major dose-limiting adverse effect is the induction of a peripheral sensory neuropathy, with cold hypersensitivity being the most frequent and the most severe symptom reported by patients (Tofthagen et al., 2011). Preclinical studies have shown that rodents, similarly to humans, develop cold allodynia (pain triggered by non-noxious cooling) as well as hyperalgesia (abnormally intense pain in response to noxious cold) after a single oxaliplatin injection (Descoeur et al., 2011; Ling et al., 2007). We therefore assessed whether *Nav1.9* expression disruption alleviates oxaliplatin-induced cold hypersensitivity with the aim of defining the potential of Nav1.9 as a drug target for the relief of cold hypersensitivity in this neuropathic state. WT and *Nav1.9*$^{-/-}$ mice were submitted to the tail immersion test at 20°C, 15°C, 10°C, and 5°C (Figure 6A). In accordance with our first observation, *Nav1.9*$^{-/-}$ mice showed an increased pain threshold at 5°C but not at higher temperatures. Four days after intraperitoneal injection of oxaliplatin (6 mg/kg), WT mice were hypersensitive to cold for every temperature tested, from 5°C to 20°C. In *Nav1.9*$^{-/-}$ mice, this symptom was significantly reduced at 5°C and 10°C, and no hypersensitivity could be detected at 15°C and 20°C. These data indicate that *Nav1.9* knockout both alleviates oxaliplatin-induced cold hyperalgesia (5°C and 10°C being considered as noxious) and abolishes cold allodynia (15°C and 20°C being non-noxious temperatures). Nav1.9 contribution to cold allodynia was confirmed with the acetone test. The gentle cooling produced by acetone evaporation under the paw induced a nociceptive behavior (licking of the paw) in WT mice treated with oxaliplatin, which was not observed in *Nav1.9*$^{-/-}$ animals (Figure 6B).

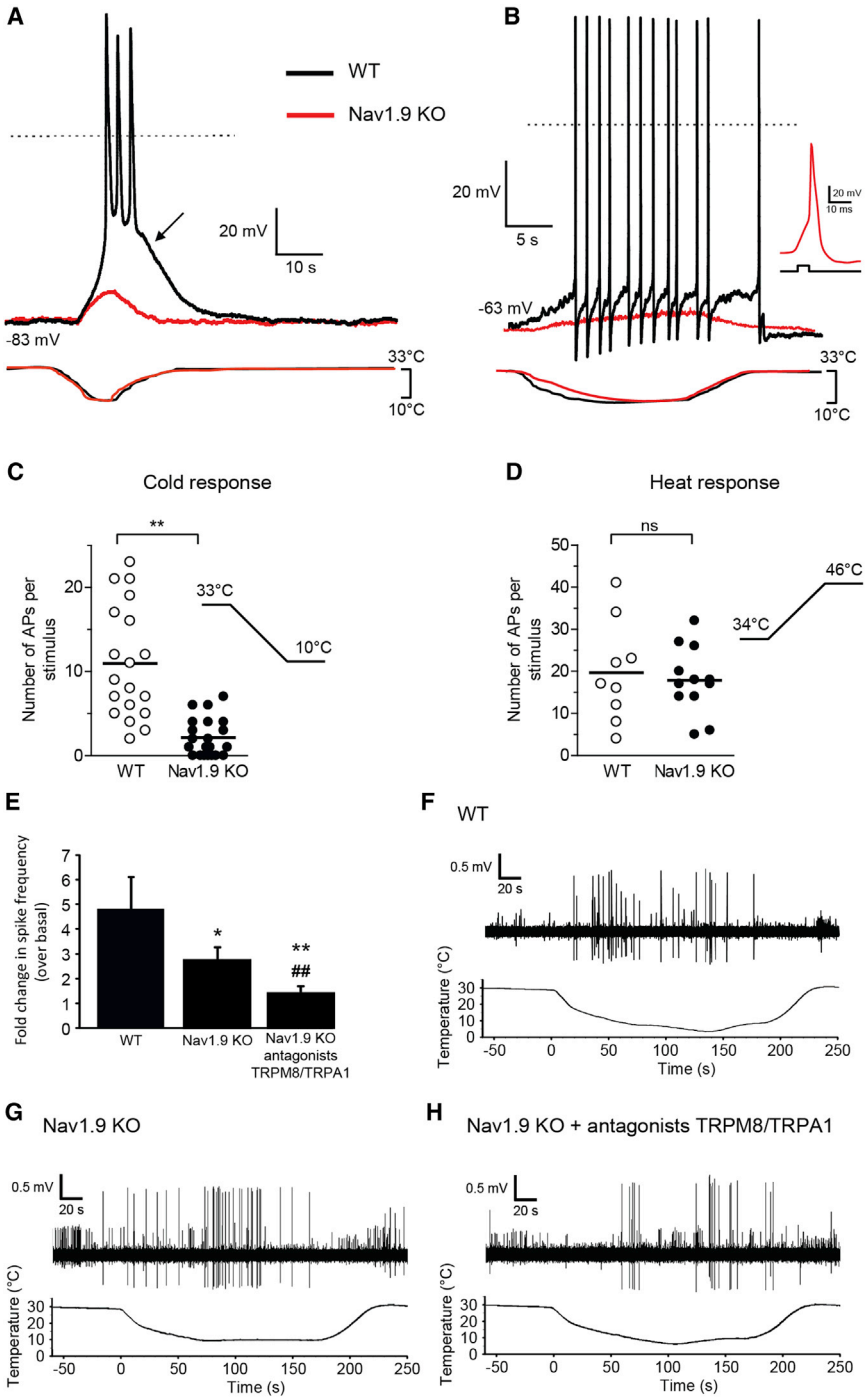

Figure 5. Nav1.9 Amplifies Cold-Induced Responses in Sensory Neurons

(A) Representative current-clamp response of a WT DRG neuron (25 pF) to a cooling ramp from 33°C to 10°C, showing a large cold-induced subthreshold depolarization and a burst of action potentials. No firing in response to cold was observed in a *Nav1.9*$^{-/-}$ neuron (31 pF) recorded under the same conditions. Steady bias currents (−70 and −83 pA in the WT and *Nav1.9*$^{-/-}$ neurons, respectively) were injected to hyperpolarize the cells to ∼−80 mV. The large regenerative depolarization (arrow) observed in the WT neuron is consistent with the presence of a large Nav1.9 current in the subthreshold voltage range. KCl-based pipette solution.

(B) Similar experiment as in (A) without the injection of a bias current (unclamped neurons). The cooling ramp elicited a small depolarization in the *Nav1.9*$^{-/-}$ neuron (29 pF), whereas it triggered sustained firing in the WT neuron (33 pF). Note that an action potential (possibly carried by Nav1.8) still occurred in the *Nav1.9*$^{-/-}$ neuron in response to a current step (right, injected current: 45 pA).

(C and D) Scatter plots showing the number of action potentials produced in response to cooling (C) or heating from 34°C to 46°C (D) in unclamped WT and *Nav1.9*$^{-/-}$ neurons that were found to respond to these stimuli. Horizontal bars indicate the mean value.

(E–H) Fold change in spike frequency of saphenous nerve fibers recorded from skin-nerve preparations, induced by the cooling of a patch of skin from 30°C to 9°C–10°C. Fibers responses are plotted as fold change of fibers activity during the cooling ramp against a control period of 60 s at 30°C. The histogram shows average fold changes recorded from WT and *Nav1.9*$^{-/-}$ mice, as well as in *Nav1.9*$^{-/-}$ mice following cutaneous application of both TRPM8 and TRPA1 blockers (10 μM BCTC and 10 μM HC-030031). Representative traces recorded in WT, in *Nav1.9*$^{-/-}$ mice and in *Nav1.9*$^{-/-}$ mice in the presence of TRPM8 and TRPA1 blockers are shown in (F), (G), and (H), respectively. Error bars correspond to SEM. *$p < 0.05$, **$p < 0.01$ versus WT, ##$p < 0.01$ versus Nav1.9 KO; ns, not significant; unpaired t test (C and D), Kruskal-Wallis test with Dunn's post-test (E).

The role played by Nav1.9 in oxaliplatin-induced cold hypersensitivity was finally assessed in knockdown rats using the paw immersion test at 5°C and 15°C. Oxaliplatin injection (6 mg/kg, intraperitoneal) resulted in cold hyperalgesia and allodynia, as shown by the reduction of the pain threshold at 5°C and 15°C (Figures 6C and 6D), in both saline and mismatch groups. No change in cold sensitivity was observed in the *Nav1.9* antisense-treated group at 5°C and 15°C, showing that knocking down *Nav1.9* expression is able to suppress both cold allodynia and hyperalgesia in this model. *Nav1.9* expression was finally assessed by quantitative PCR (qPCR) in the lumbar DRGs of oxaliplatin-treated rats, and no difference could be detected compared to vehicle-treated rats (Figure S5).

DISCUSSION

Our data provide evidence for a specialized role of Nav1.9 in cold-triggered nociception. We show that Nav1.9 channels display enhanced activity in cold-sensitive neurons. We

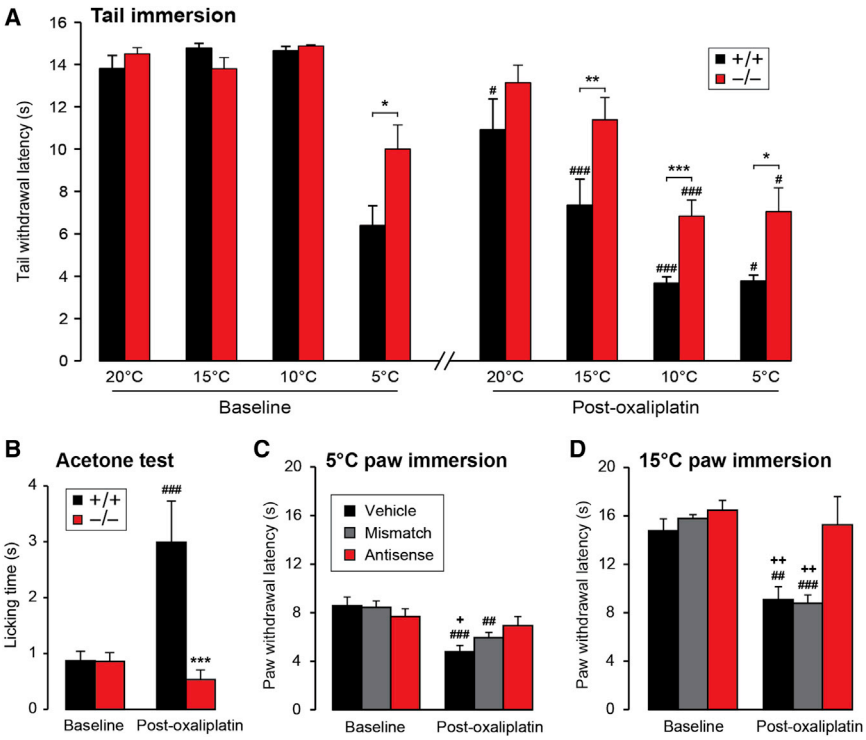

Figure 6. Disrupting *Nav1.9* Expression Alleviates Oxaliplatin-Induced Cold Hypersensitivity in Mice and Rats

(A) Cold pain thresholds of WT and *Nav1.9*$^{-/-}$ mice subjected to the tail immersion test at temperatures ranging from 5°C to 20°C before and 4 days following intraperitoneal injection of oxaliplatin (6 mg/kg). n = 8.

(B) Cold allodynia, characterized by an increase in paw licking in response to gentle acetone-mediated cooling, was observed in WT but not in *Nav1.9*$^{-/-}$ mice. n = 8.

(C and D) Cold pain thresholds of *Nav1.9* knockdown rats subjected to the 5°C (D) or 15°C (D) paw immersion test, before and 3 days following intraperitoneal injection of oxaliplatin (6 mg/kg). n = 8. $^{*}p < 0.05$, $^{**}p < 0.01$, $^{***}p < 0.001$ versus +/+; $^{\#}p < 0.05$, $^{\#\#}p < 0.01$, $^{\#\#\#}p < 0.001$ versus baseline; $^{+}p < 0.05$, $^{++}p < 0.01$ versus antisense; $^{\#\#}p < 0.01$, $^{\#\#\#}p < 0.001$ versus baseline; two-way ANOVA followed by Student-Newman-Keuls' test. Error bars correspond to SEM.

also establish that Nav1.9 serves as a subthreshold amplifier of cold transducer signals, thereby promoting firing in response to noxious cold. Moreover, the disruption of *Nav1.9* expression increases cold-induced pain thresholds in healthy rodents and reduces or suppresses cold hyperalgesia and allodynia in rodents suffering from oxaliplatin-induced peripheral neuropathy.

Nav1.9 was known to be involved in mechanical and heat hypersensitivity following inflammation (Amaya et al., 2006; Ligonnier et al., 2011), but no physiological mechano-sensory or thermo-sensory phenotype has been documented to date. We show that this channel is involved in the perception of pain triggered by cold in the noxious range, as supported by the alteration of nociceptive reflexes (tail and paw immersion tests) as well as integrated behaviors (thermal preference test, cold ramp test) in animals deficient for *Nav1.9*. According to a previous study (Amaya et al., 2006), we observed no difference in the number of flinches over 5 min or in the latency to flinching behavior between WT and *Nav1.9*$^{-/-}$ mice placed on a 0°C cold plate. This type of behavior has later been shown to be possibly characteristic of thermal discrimination rather than cold nociception (Karashima et al., 2009). In regard to these findings and as *Nav1.9*$^{-/-}$ mice kept avoiding the cold plate during the 21 versus 12°C thermal preference test (spending less than 19% of the time on this plate) but spent more time exploring it than WTs (11.6%), we propose that Nav1.9 is specifically required for cold nociception but not for thermal discrimination.

As changes in the expression of other genes involved in cold nociception could be indirectly responsible for the phenotype observed in *Nav1.9*$^{-/-}$ mice, we performed acute *Nav1.9* knockdown in rats. Rats treated with *Nav1.9* antisense ODNs have higher pain thresholds to noxious cold, as observed in *Nav1.9* null mice. Moreover, the channels involved in cold sensitivity in vivo, TRPM8, TRPA1, Nav1.8, TREK-1, and TRAAK showed similar expression levels in WT and *Nav1.9*$^{-/-}$ mice. Collectively, these data favor the view that the phenotype observed in *Nav1.9*$^{-/-}$ mice is not imputable to developmental changes affecting the expression of known cold transducers but is rather directly caused by the lack of functional Nav1.9 channels in sensory neurons. In vitro experiments revealed that Nav1.9 activity is specifically enhanced in a subset of cold-sensitive neurons, which do not seem to require TRPA1 or TRPM8 as cold transducers. Although we cannot exclude the possibility that Nav1.9 contributes to some extend to cold responses in a few TRPM8- and/or TRPA1 nerve fibers, our data indicate that cold transduction in Nav1.9-positive nociceptive fibers uses a yet unknown cold sensor. This inference is supported by a recent study showing negative correlation between TRPM8 and both Nav1.9 and TRPA1 expression levels in sensory neurons (Morenilla-Palao et al., 2014), TRPM8-positive neurons relying on TASK-3 expression for normal response to cooling.

The observation that large basal Nav1.9 activity was detected in cold-sensitive neurons in the absence of exogenous modulators of Nav1.9 channels (e.g., internal fluoride) (Coste et al., 2004; Maingret et al., 2008) indicates that these neurons contain constitutive modulators of Nav1.9 activity. Nav1.9 exhibits unique electrophysiological properties that enable it to produce a persistent Na^{+} current (Coste et al., 2004; Cummins et al., 1999) and to contribute to the setting of the electrogenic properties of nociceptive neurons by amplifying their responses to subthreshold stimuli (Coste et al., 2004; Herzog et al., 2001; Maingret et al., 2008). The picture that emerges from our study is that in cold-sensitive nociceptors, active Nav1.9 channels evoke a regenerative response near rest, which amplifies the

cold transducer depolarization and drives neuronal excitability at low temperatures. As Nav1.8-generated action potentials are resistant to cooling, they are ideally suited to arise from Nav1.9-amplified subthreshold depolarizations. The combination of Nav1.9 and Nav1.8 channels, whose expression patterns largely overlap (Amaya et al., 2000), provides an ideal environment for the transmission of cold nociceptive information to the central nervous system. The cold-sensitive potassium channel TREK-2 has also been reported to be strongly co-localized with Nav1.9 in IB4-positive neurons, in which it contributes actively to the setting of a particularly hyperpolarized resting membrane potential (Acosta et al., 2014). In these neurons, TREK-2 might increase Nav1.9 availability to respond to cold-transducer depolarizations by setting a hyperpolarized membrane potential at physiological temperature while being closed upon cooling.

We finally show that the role played by Nav1.9 in cold nociception could be exploited with the idea of relieving pathological cold pain hypersensitivity. Our results show that the disruption of *Nav1.9* expression in mice or rats efficiently alleviates the pathological hypersensitivity to cold induced by oxaliplatin. Cold hyperalgesia was reduced in *Nav1.9*$^{-/-}$ mice and suppressed in rats treated with *Nav1.9* antisense ODNs, but most remarkably, oxaliplatin-induced cold allodynia was completely absent in *Nav1.9*$^{-/-}$ mice and knockdown rats. Our results therefore identify Nav1.9 as a potential drug target for the treatment of oxaliplatin-induced cold allodynia. Nav1.9 has also previously been shown to play a role in cold allodynia induced by chronic constriction injury and spared nerve injury (Leo et al., 2010), suggesting that Nav1.9 could play a role in cold allodynia in diverse pathological conditions. However, another study has shown no relief of cold allodynia in *Nav1.9*$^{-/-}$ mice following spared nerve injury and partial sciatic nerve injury (Amaya et al., 2006), and more work is required to fully characterize the contribution of Nav1.9 to neuropathic pain.

In conclusion, we provide evidence for a major contribution of Nav1.9 channels to normal and pathological cold pain signaling. The relative cold resistance of Nav1.9, together with its functional upregulation in a subset of cold-sensitive sensory neurons, are decisive properties making this channel—along with Nav1.8—crucial for cold nociception. In addition, Nav1.9 may be an interesting drug target for the treatment of painful cold hypersensitivity associated with oxaliplatin-based chemotherapies.

EXPERIMENTAL PROCEDURES

Animals and In Vivo Procedures

Animals were used in accordance with the European Community guiding in the care and use of animals (86/609/CEE), and the guidelines of the Committee for Research and Ethical Issues of the International Association for the Study of Pain (Zimmermann, 1983) were followed. Behavioral tests and pain models were all approved by the ethics committee of Auvergne (Comité Régional d'Ethique en Matière d'Expérimentation Animale Auvergne).

Nav1.9$^{-/-}$ and *Nav1.8*$^{-/-}$ mice were generated from a C57Bl6/J background as previously described (Maingret et al., 2008; Osorio et al., 2014). Behavioral experiments were performed blind to genotype on WT and *Nav1.9*$^{-/-}$ male littermates (8–14 weeks). Experiments that did not require the use of knockout animals were done on 20–24 g C57Bl6/J male mice (Charles River).

Antisense studies were performed with 150–175 g male Sprague Dawley rats (Charles River). Prior to experiments, animals received six intrathecal injections, one every 12 hr, of saline, 12.5 μg mismatch (5′-GCCTTGTCTTTGG ACTTCTTC-3′) or antisense ODNs targeting *Nav1.9* mRNA (5′-GCTCTGTT CTTGAGCTTTCTC-3′) in 10 μl saline (Porreca et al., 1999).

Icilin and cinnamaldehyde were injected subplantarly, both at 14 mM in 25 μl vehicle. Icilin was diluted in saline containing 50% dimethylsulfoxide, and cinnamaldehyde was diluted in saline containing 0.5% tween-80. Toxin-free vehicle injections were performed in WT animals to ensure that no nociceptive behavior was induced by these solutions. Peripheral neuropathy was induced in mice and rats by a single intraperitoneal injection of oxaliplatin at 6 mg/kg. Oxaliplatin was diluted to 1 mg/ml in 5% glucose.

Animals were not involved in more than one test, except for oxaliplatin-treated mice, which underwent both tail immersion and acetone test in the morning and afternoon of day 4, respectively, and rats, which underwent 15°C and 5°C paw immersion in the morning and afternoon of day 3, respectively.

Behavioral Tests

Tail/Paw Immersion Test

Animals were held in a piece of cloth and two-thirds of the tail, or the hind paw up to the ankle, were immersed in a thermostatically controlled water bath until shaking or withdrawal was observed. The first two measurements not differing by more than a second were averaged and assigned as the pain threshold. A cutoff time of 15 s for mice and 30 s for rats was applied.

Thermal Preference Test

The thermal preference test (Bioseb) consists of two adjacent plates: the reference plate set at 25°C and the test plate set at 21°C or 12°C. Mice were placed on one plate in the dark and allowed to explore both plates for 3 min. The time spent on the test plate was monitored using an infrared video camera. The next day, mice were placed on the same plate, the temperatures of the plates being inverted. Values obtained on both days were averaged.

Dynamic Cold Plate

Mice were placed on a plate (Bioseb) set at a temperature decreasing from 25°C to 0°C at a 1°C • min^{-1} rate. The experiment was performed in the dark, and nocifensive behavior (jumps) was followed using an infrared video camera.

Acetone Test

80 μl of acetone at room temperature were applied under the hind paw and the time spent by the animals shaking or licking their paw was measured over a 30 s period.

Dissociation of DRG and Cell Culture

Cultures of sensory neurons were performed as previously described (Hao and Delmas, 2010; Hao et al., 2013). Briefly, DRGs were removed and incubated in Hank's balanced salt solution containing 2 mg/ml collagenase IA for 35–45 min at 37°C. DRGs were cultured in DMEM supplemented with 10% heat-inactivated fetal calf serum, 50 U/ml penicillin-streptomycin, 2 mM L-glutamine, 25 mM glucose, 25 ng/ml nerve growth factor, and 2 ng/ml glial-derived neurotrophic factor.

Electrophysiology

Patch Clamp

Sodium currents were recorded using either CsF- or CsCl-based pipette solutions as indicated. The CsF-containing solution is optimal to record Nav1.9 currents (Coste et al., 2004, 2007; Maingret et al., 2008) and consisted of (in mM) 100 CsCl, 30 CsF, 5 NaCl, 2.4 $CaCl_2$, 1 $MgCl_2$, 5 ethyleneglycotetraacetic acid (EGTA), 10 4-(2-hydroxyethyl)-1-piperazineethanesulfonic acid (HEPES), 4 adenosine triphosphate (MgATP), 0.4 guanosine triphosphate (NaGTP) (pH adjusted to 7.3 with CsOH, 301 mOsm/l). CsCl-pipette solution consisted of (mM) 130 CsCl, 5 NaCl, 2.4 $CaCl_2$, 1 $MgCl_2$, 5 EGTA, 10 HEPES, 4 MgATP, 0.4 NaGTP (pH adjusted to 7.3 with CsOH, 303 mOsm/l). To improve voltage clamp conditions when recording Na^+ currents, the extracellular solution had a reduced concentration for Na^+ (in mM): 100 choline-chloride, 40 NaCl, 3 KCl, 2.5 $CaCl_2$, 1 $MgCl_2$, 10 HEPES, 10 glucose, supplemented with 300 nM TTX, 5 μM $LaCl_3$ and 1 mM amiloride (pH 7.35, 308 mOsm/l) (Coste et al., 2007). KCl-based pipette solution contained (mM) 134 KCl, 10 HEPES, 4 MgATP,

0.4 NaGTP, 1 $MgCl_2$, 2.4 $CaCl_2$, and 5 EGTA (pH adjusted to 7.3 with KOH, 296 mOsm/l). The standard external solution consisted of (mM) 132 NaCl, 1 KCl, 1 $MgCl_2$, 2.5 $CaCl_2$, 10 HEPES, 5 μM $LaCl_3$, and 10 D-glucose (pH adjusted to 7.3 with NaOH, 300 mOsm/l). Each neuron was subjected to a single thermal stimulus. In Figures 2G and 2H, cold-induced currents were recorded at −60 mV using the KCl-based pipette solution, whereas in Figure 4, cold- and heat-induced currents were recorded using Cs^+-based pipette solutions.

Skin-Nerve Preparation

The skin-nerve preparation was used as previously described (Reeh, 1986; Zimmermann et al., 2009). Adult mice, 8 to 12 weeks old, were killed with CO_2. The saphenous nerve and the skin of the hind limb were dissected and placed in an organ bath. The chamber was perfused with warm, 30°C–31°C, synthetic interstitial fluid (SIF buffer) consisting of (in mM) 120 NaCl, 3.5 KCl, 0.7 $MgSO_4$, 1.7 NaH_2PO_4, 5 Na_2HCO_3, 2 $CaCl_2$, 9.5 Na-Gluconate, 5.5 glucose, 7.5 sucrose, and 10 HEPES at a pH of 7.4. The skin was placed with the corium side up in the organ bath and the nerve was placed in an adjacent chamber for recording. The nerve was gently teased, and groups of nerve fibers were placed on the gold recording electrode. A patch of skin was isolated from the surrounding bath with a plastic ring of 1 cm diameter and continuously perfused with SIF at a temperature controlled with a CL-100 temperature controller (Warner Instrument). The isolated patch of skin was cooled from 30°C–31°C to 9°C–10°C in 180 s. In *Nav1.9*$^{-/-}$ mice, a second ramp was applied following application of the TRPM8 and TRPA1 antagonists BCTC (10 μM) and HC-030031 (10 μM) through the temperature controller. Control experiments showed that successive applications of cooling ramps elapsed by at least 10 min did not cause significant desensitization of the cold responses. Raw electrophysiological data were recorded with an AC differential amplifier DAM 80 (WPI) and Spike2 software (Cambridge Electronic Design). Spikes were discriminated off-line with the Spike2 software and visualized individually to detect false positives.

Measurement of Cytosolic [Ca^{2+}]

DRG neurons were loaded with 2 μM Fura-PE3-AM in culture medium for 30 min. Glass coverslips were then individually inserted in a specific chamber and placed on the stage of an inverted epifluorescence microscope (Olympus IX71) equipped with a ×10 UPLSAPO objective. Fura-PE3 was alternately excited at 345 and 380 nm, and ratios of the resulting images (345/380) were produced every 400 ms. Digital images were sampled at a 12-bit resolution by a fast-scan, cooled charge-coupled device (B/W CCD) digital camera (Orca-ER, Hamamatsu). $[Ca^{2+}]_i$ was calculated using a molecular probes kit (Calcium Calibration Buffer Kit 1, C3008MP; Invitrogen) and the equation $[Ca^{2+}]_i = K_d \{(R - R_{min})/(R_{max} - R)\}$, where R is the measured ratio intensity, R_{min} and R_{max} are the minimum and the maximum of ratios, and K_d is the dissociation constant of the Fura-PE3 dye. R_{min} and R_{max} were determined by exposing cells to a zero Ca^{2+}/ionomycin (5 μM) solution and to a 10 mM Ca^{2+}/ionomycin (5 μM) solution, respectively.

RNA Extraction and RT-qPCR

RNA was isolated from snap frozen T12 to L6 DRGs using the RNeasy mini kit (QIAGEN) according to the manufacturer's instruction, including a DNase I treatment step. 1 μg RNA was used for reverse transcription using the SuperScript II Reverse Transcriptase (Invitrogen) according to the supplier's procedure. Real-time PCR was performed on a Mastercycler ep realplex (Eppendorf). Samples were run in triplicate in a 6.3 μl volume containing 1.3 μl of 1/40 cDNA dilution, 0.5 μM primers, 3 mM $MgCl_2$, and LightCycler Fast-Start SYBR Green reaction mix (Roche). Optimal annealing temperature was preliminarily determined by gradient qPCR and subsequent electrophoresis. The primers used were the following from 5′ to 3′: TGTGCATCTACATGCTCTCCACCA (F) and GGGATGTT TAGGCGGTTGCAGTA (R) for mouse *TRPM8* (NM_134252, 157 bp), CAGCCAA GGAGCAAATCCAAACCT (F) and GGACATCAAAGCCGTGTTCCCATT (R) for mouse *TRPA1* (NM_177781, 160 bp), AACTTCGACAACGTTGCTATGGGC (F) and ACATGTACAGGCTCTCCTCCCAAT (F) for mouse *Nav1.8* (NM_009134, 139 bp), CCCAAGTCTGCTGCTCAGAACT (F) and ACGGTGGGTTTTGAGGA GAAT (R) for mouse *TREK-1* (NM_010607, 59 bp), CTCTGGAGCAGCCTCACGA (F) and TCGGCCATGATCCATTTTCT (R) for mouse *TRAAK* (NM_008431, 53 bp), TTGCTGACCTGCTGGATTAC (F) and AGTTGAGAGATCATCTCCAC (R) for mouse *HPRT* (NM_013556, 149 bp). Relative amounts of cDNA were calculated as a function of the cycle thresholds (Ct) using a standard concentration curve obtained from a serial dilution (1/10 to 1/640) of a mix of the cDNA samples. For each sample, the relative amount of the gene of interest cDNA was normalized by the amount of *HPRT* cDNA.

In Situ Hybridization

Mice were deeply anesthetized with sodium pentobarbital (100 mg/kg intraperitoneal) and transcardially perfused with 10 ml 0.9% NaCl followed by 40 ml ice-cold 4% paraformaldehyde in PBS. Lumbar DRGs were collected and post-fixed in PBS 4% paraformaldehyde for 4 hr before incubation in PBS 30% sucrose for 12 hr. Tissues were embedded in Tissue-Tek OCT medium and frozen and stored at −80°C until serial cryostat sections (12 μm) were prepared and mounted onto SuperFrost slides.

cRNA probes targeting *Nav1.9*, *TRPM8*, and *TRPA1* were transcribed using cDNA templates amplified by nested PCR from mouse DRGs cDNA. A T7 promoter sequence was added to the internal reverse primer to allow in vitro transcription of the PCR product. The following primers were used from 5′ to 3′: CTCTTTGATGAGCACGTGGA (F1), CTTGTATCCAGGGTGGCTGT (R1), AAAA TCCCAGGAGCCTTGTT (F2) and TAATACGACTCACTATAGGGACCACCATG ATCAGCACAAA (T7-R2) for *Nav1.9* (NM_134252.3, 769 bp from 2034 to 2802); CCAGCAAGCTTCTGAAGACC (F1), ATCTCCAGCGCTGTTCATTT (R1), ATG AATATGAGACCCGAGCAGT (F2), and TAATACGACTCACTATAGGGGCAAA GAGGAACAGGAAGAAGA (T7-R2) for *TRPM8* (NM_011887.3, 750 bp from 1657 to 2406); ACCCATGACCCTTCTTGTTG (F1), TTCCAGCCTCTCCTT CTTGA (R1); AGTATCATCTTCGTGTTGCCCT (F2) and TAATACGACTCACTA TAGGGGTGAGGTCCTTCAGCCGATA (T7-R2) for *TRPA1* (NM_177781.4, 719 bp from 3197 to 1657). cRNA probes were synthesized by in vitro transcription of the PCR templates using T7 RNA polymerase (Promega), incorporating either digoxigenin-UTP or biotin-UTP (Roche). cRNA probes were subsequently purified and stored at −80°C until use.

For in situ hybridization, slices were permeabilized using proteinase K, treated with 0.1 M triethanolamine and acetic anhydre, and incubated in prehybridization buffer (50% formamide, 5× saline-sodium citrate, 5× Denhardt's solution, 250 μg/ml yeast tRNA and 500 μg/ml herring/salmon sperm DNA) for 3 hr at room temperature prior to hybridization overnight at 55°C. Digoxigenin-labeled Nav1.9 cRNA was used in combination with either biotin-labeled TRPM8 cRNA or biotin-labeled TRPA1 cRNA. Digoxigenin-labeled TRPM8 cRNA was used in combination with biotin-labeled TRPA1 cRNA. Probes were targeted by POD (horseradish peroxidase)-conjugated antibodies to biotin or digoxigenin (Roche, 1:500) and detected by fluorescence using Tyramide Signal Amplification (TSA PLUS kit; Perkin Elmer) according to the manufacturer's instructions. Slices were treated with H_2O_2 before adding the second POD-conjugated antibody to inactivate the first POD peroxydase.

Statistics

Raw data were analyzed for statistical significance using either one-way ANOVA followed by Bonferroni multiple comparisons versus control group, two-way ANOVA followed by Student-Newman-Keuls all pairwise multiple comparison procedure, unpaired t test, or Mann-Whitney test depending on the experimental design, using SigmaPlot and Prism software. All values are shown as mean ± SEM.

SUPPLEMENTAL INFORMATION

Supplemental Information includes Supplemental Experimental Procedures and five figures and can be found with this article online at http://dx.doi.org/10.1016/j.celrep.2015.04.027.

AUTHOR CONTRIBUTIONS

S.L. carried out the behavioral and molecular studies on mice, analyzed the data, and wrote the paper. C.B., M.A, and C.G. performed electrophysiology. L.R.-D. and F.P. performed calcium imaging. J.N., J.R., and V.B. performed skin nerve experiments. J.F. and Y.A. were involved in molecular studies. E.C. performed the behavioral studies on rats. L.P. was involved in behavioral studies on mice. A.E., P.D., and J.B. supervised the project and wrote the paper.

ACKNOWLEDGMENTS

We thank Aziz Moqrich for the help provided with setting up in situ hybridization experiments, James J. Cox for pertinent advice and proofreading of the article, and Axel Fernandez for excellent technical assistance. This study was funded by grants from the Agence Nationale de la Recherche (ANR-08-MNPS-025-02, ANR-09-MNPS-037-01 to P.D.), Fondation pour la Recherche Médicale (FRM 2013 DEQ20130326482 to P.D.), ARC/INCa (to J.B., A.E., and P.D.), CNRS, INSERM, Aix-Marseille Université and Université d'Auvergne. M.A. was supported by fellowship from Fondation pour la Recherche Médicale. S.L. was supported by fellowships from Ministère de l'Enseignement Supérieur et de la Recherche and La Ligue contre le cancer.

Received: August 1, 2014
Revised: January 16, 2015
Accepted: April 13, 2015
Published: May 7, 2015

REFERENCES

Acosta, C., Djouhri, L., Watkins, R., Berry, C., Bromage, K., and Lawson, S.N. (2014). TREK2 expressed selectively in IB4-binding C-fiber nociceptors hyperpolarizes their membrane potentials and limits spontaneous pain. J. Neurosci. *34*, 1494–1509.

Amaya, F., Decosterd, I., Samad, T.A., Plumpton, C., Tate, S., Mannion, R.J., Costigan, M., and Woolf, C.J. (2000). Diversity of expression of the sensory neuron-specific TTX-resistant voltage-gated sodium ion channels SNS and SNS2. Mol. Cell. Neurosci. *15*, 331–342.

Amaya, F., Wang, H., Costigan, M., Allchorne, A.J., Hatcher, J.P., Egerton, J., Stean, T., Morisset, V., Grose, D., Gunthorpe, M.J., et al. (2006). The voltage-gated sodium channel Na(v)1.9 is an effector of peripheral inflammatory pain hypersensitivity. J. Neurosci. *26*, 12852–12860.

Baker, M.D., Chandra, S.Y., Ding, Y., Waxman, S.G., and Wood, J.N. (2003). GTP-induced tetrodotoxin-resistant Na+ current regulates excitability in mouse and rat small diameter sensory neurones. J. Physiol. *548*, 373–382.

Bautista, D.M., Jordt, S.-E., Nikai, T., Tsuruda, P.R., Read, A.J., Poblete, J., Yamoah, E.N., Basbaum, A.I., and Julius, D. (2006). TRPA1 mediates the inflammatory actions of environmental irritants and proalgesic agents. Cell *124*, 1269–1282.

Bautista, D.M., Siemens, J., Glazer, J.M., Tsuruda, P.R., Basbaum, A.I., Stucky, C.L., Jordt, S.-E., and Julius, D. (2007). The menthol receptor TRPM8 is the principal detector of environmental cold. Nature *448*, 204–208.

Chen, J., Kang, D., Xu, J., Lake, M., Hogan, J.O., Sun, C., Walter, K., Yao, B., and Kim, D. (2013). Species differences and molecular determinant of TRPA1 cold sensitivity. Nat. Commun. *4*, 2501.

Coste, B., Osorio, N., Padilla, F., Crest, M., and Delmas, P. (2004). Gating and modulation of presumptive NaV1.9 channels in enteric and spinal sensory neurons. Mol. Cell. Neurosci. *26*, 123–134.

Coste, B., Crest, M., and Delmas, P. (2007). Pharmacological dissection and distribution of NaN/Nav1.9, T-type Ca2+ currents, and mechanically activated cation currents in different populations of DRG neurons. J. Gen. Physiol. *129*, 57–77.

Cummins, T.R., Dib-Hajj, S.D., Black, J.A., Akopian, A.N., Wood, J.N., and Waxman, S.G. (1999). A novel persistent tetrodotoxin-resistant sodium current in SNS-null and wild-type small primary sensory neurons. J. Neurosci. *19*, RC43.

Descoeur, J., Pereira, V., Pizzoccaro, A., Francois, A., Ling, B., Maffre, V., Couette, B., Busserolles, J., Courteix, C., Noel, J., et al. (2011). Oxaliplatin-induced cold hypersensitivity is due to remodelling of ion channel expression in nociceptors. EMBO Mol. Med. *3*, 266–278.

Dhaka, A., Murray, A.N., Mathur, J., Earley, T.J., Petrus, M.J., and Patapoutian, A. (2007). TRPM8 is required for cold sensation in mice. Neuron *54*, 371–378.

Fukuoka, T., Kobayashi, K., Yamanaka, H., Obata, K., Dai, Y., and Noguchi, K. (2008). Comparative study of the distribution of the alpha-subunits of voltage-gated sodium channels in normal and axotomized rat dorsal root ganglion neurons. J. Comp. Neurol. *510*, 188–206.

Gentry, C., Stoakley, N., Andersson, D.A., and Bevan, S. (2010). The roles of iPLA2, TRPM8 and TRPA1 in chemically induced cold hypersensitivity. Mol. Pain *6*, 4.

Hao, J., and Delmas, P. (2010). Multiple desensitization mechanisms of mechanotransducer channels shape firing of mechanosensory neurons. J. Neurosci. *30*, 13384–13395.

Hao, J., Padilla, F., Dandonneau, M., Lavebratt, C., Lesage, F., Noël, J., and Delmas, P. (2013). Kv1.1 channels act as mechanical brake in the senses of touch and pain. Neuron *77*, 899–914.

Hao, J., Bonnet, C., Amsalem, M., Ruel, J., and Delmas, P. (2015). Transduction and encoding sensory information by skin mechanoreceptors. Pflugers Arch. *467*, 109–119.

Herzog, R.I., Cummins, T.R., and Waxman, S.G. (2001). Persistent TTX-resistant Na+ current affects resting potential and response to depolarization in simulated spinal sensory neurons. J. Neurophysiol. *86*, 1351–1364.

Karashima, Y., Talavera, K., Everaerts, W., Janssens, A., Kwan, K.Y., Vennekens, R., Nilius, B., and Voets, T. (2009). TRPA1 acts as a cold sensor in vitro and in vivo. Proc. Natl. Acad. Sci. USA *106*, 1273–1278.

Kiernan, M.C. (2007). The pain with platinum: oxaliplatin and neuropathy. Eur. J. Cancer *43*, 2631–2633.

Knowlton, W.M., Palkar, R., Lippoldt, E.K., McCoy, D.D., Baluch, F., Chen, J., and McKemy, D.D. (2013). A sensory-labeled line for cold: TRPM8-expressing sensory neurons define the cellular basis for cold, cold pain, and cooling-mediated analgesia. J. Neurosci. *33*, 2837–2848.

Kobayashi, K., Fukuoka, T., Obata, K., Yamanaka, H., Dai, Y., Tokunaga, A., and Noguchi, K. (2005). Distinct expression of TRPM8, TRPA1, and TRPV1 mRNAs in rat primary afferent neurons with adelta/c-fibers and colocalization with trk receptors. J. Comp. Neurol. *493*, 596–606.

Kwan, K.Y., Allchorne, A.J., Vollrath, M.A., Christensen, A.P., Zhang, D.-S., Woolf, C.J., and Corey, D.P. (2006). TRPA1 contributes to cold, mechanical, and chemical nociception but is not essential for hair-cell transduction. Neuron *50*, 277–289.

Leo, S., D'Hooge, R., and Meert, T. (2010). Exploring the role of nociceptor-specific sodium channels in pain transmission using Nav1.8 and Nav1.9 knockout mice. Behav. Brain Res. *208*, 149–157.

Ling, B., Coudoré-Civiale, M.-A., Balayssac, D., Eschalier, A., Coudoré, F., and Authier, N. (2007). Behavioral and immunohistological assessment of painful neuropathy induced by a single oxaliplatin injection in the rat. Toxicology *234*, 176–184.

Lolignier, S., Amsalem, M., Maingret, F., Padilla, F., Gabriac, M., Chapuy, E., Eschalier, A., Delmas, P., and Busserolles, J. (2011). Nav1.9 channel contributes to mechanical and heat pain hypersensitivity induced by subacute and chronic inflammation. PLoS ONE *6*, e23083.

Maingret, F., Coste, B., Padilla, F., Clerc, N., Crest, M., Korogod, S.M., and Delmas, P. (2008). Inflammatory mediators increase Nav1.9 current and excitability in nociceptors through a coincident detection mechanism. J. Gen. Physiol. *131*, 211–225.

Maruyama, H., Yamamoto, M., Matsutomi, T., Zheng, T., Nakata, Y., Wood, J.N., and Ogata, N. (2004). Electrophysiological characterization of the tetrodotoxin-resistant Na+ channel, Na(v)1.9, in mouse dorsal root ganglion neurons. Pflugers Arch. *449*, 76–87.

McKemy, D.D., Neuhausser, W.M., and Julius, D. (2002). Identification of a cold receptor reveals a general role for TRP channels in thermosensation. Nature *416*, 52–58.

Moparthi, L., Survery, S., Kreir, M., Simonsen, C., Kjellbom, P., Högestätt, E.D., Johanson, U., and Zygmunt, P.M. (2014). Human TRPA1 is intrinsically cold- and chemosensitive with and without its N-terminal ankyrin repeat domain. Proc. Natl. Acad. Sci. USA *111*, 16901–16906.

Morenilla-Palao, C., Luis, E., Fernández-Peña, C., Quintero, E., Weaver, J.L., Bayliss, D.A., and Viana, F. (2014). Ion channel profile of TRPM8 cold receptors

reveals a role of TASK-3 potassium channels in thermosensation. Cell Rep. *8*, 1571–1582.

Munns, C., AlQatari, M., and Koltzenburg, M. (2007). Many cold sensitive peripheral neurons of the mouse do not express TRPM8 or TRPA1. Cell Calcium *41*, 331–342.

Noël, J., Zimmermann, K., Busserolles, J., Deval, E., Alloui, A., Diochot, S., Guy, N., Borsotto, M., Reeh, P., Eschalier, A., and Lazdunski, M. (2009). The mechano-activated K+ channels TRAAK and TREK-1 control both warm and cold perception. EMBO J. *28*, 1308–1318.

Osorio, N., Korogod, S., and Delmas, P. (2014). Specialized functions of Nav1.5 and Nav1.9 channels in electrogenesis of myenteric neurons in intact mouse ganglia. J. Neurosci. *34*, 5233–5244.

Padilla, F., Couble, M.-L., Coste, B., Maingret, F., Clerc, N., Crest, M., Ritter, A.M., Magloire, H., and Delmas, P. (2007). Expression and localization of the Nav1.9 sodium channel in enteric neurons and in trigeminal sensory endings: implication for intestinal reflex function and orofacial pain. Mol. Cell. Neurosci. *35*, 138–152.

Peier, A.M., Moqrich, A., Hergarden, A.C., Reeve, A.J., Andersson, D.A., Story, G.M., Earley, T.J., Dragoni, I., McIntyre, P., Bevan, S., and Patapoutian, A. (2002). A TRP channel that senses cold stimuli and menthol. Cell *108*, 705–715.

Pereira, V., Busserolles, J., Christin, M., Devilliers, M., Poupon, L., Legha, W., Alloui, A., Aissouni, Y., Bourinet, E., Lesage, F., et al. (2014). Role of the TREK2 potassium channel in cold and warm thermosensation and in pain perception. Pain *155*, 2534–2544.

Pogorzala, L.A., Mishra, S.K., and Hoon, M.A. (2013). The cellular code for mammalian thermosensation. J. Neurosci. *33*, 5533–5541.

Porreca, F., Lai, J., Bian, D., Wegert, S., Ossipov, M.H., Eglen, R.M., Kassotakis, L., Novakovic, S., Rabert, D.K., Sangameswaran, L., and Hunter, J.C. (1999). A comparison of the potential role of the tetrodotoxin-insensitive sodium channels, PN3/SNS and NaN/SNS2, in rat models of chronic pain. Proc. Natl. Acad. Sci. USA *96*, 7640–7644.

Priest, B.T., Murphy, B.A., Lindia, J.A., Diaz, C., Abbadie, C., Ritter, A.M., Liberator, P., Iyer, L.M., Kash, S.F., Kohler, M.G., et al. (2005). Contribution of the tetrodotoxin-resistant voltage-gated sodium channel NaV1.9 to sensory transmission and nociceptive behavior. Proc. Natl. Acad. Sci. USA *102*, 9382–9387.

Reeh, P.W. (1986). Sensory receptors in mammalian skin in an in vitro preparation. Neurosci. Lett. *66*, 141–146.

Sarria, I., Ling, J., and Gu, J.G. (2012). Thermal sensitivity of voltage-gated Na+ channels and A-type K+ channels contributes to somatosensory neuron excitability at cooling temperatures. J. Neurochem. *122*, 1145–1154.

Story, G.M., Peier, A.M., Reeve, A.J., Eid, S.R., Mosbacher, J., Hricik, T.R., Earley, T.J., Hergarden, A.C., Andersson, D.A., Hwang, S.W., et al. (2003). ANKTM1, a TRP-like channel expressed in nociceptive neurons, is activated by cold temperatures. Cell *112*, 819–829.

Tofthagen, C., McAllister, R.D., and McMillan, S.C. (2011). Peripheral neuropathy in patients with colorectal cancer receiving oxaliplatin. Clin. J. Oncol. Nurs. *15*, 182–188.

Zimmermann, M. (1983). Ethical guidelines for investigations of experimental pain in conscious animals. Pain *16*, 109–110.

Zimmermann, K., Leffler, A., Babes, A., Cendan, C.M., Carr, R.W., Kobayashi, J., Nau, C., Wood, J.N., and Reeh, P.W. (2007). Sensory neuron sodium channel Nav1.8 is essential for pain at low temperatures. Nature *447*, 855–858.

Zimmermann, K., Hein, A., Hager, U., Kaczmarek, J.S., Turnquist, B.P., Clapham, D.E., and Reeh, P.W. (2009). Phenotyping sensory nerve endings in vitro in the mouse. Nat. Protoc. *4*, 174–196.

Zimmermann, K., Lennerz, J.K., Hein, A., Link, A.S., Kaczmarek, J.S., Delling, M., Uysal, S., Pfeifer, J.D., Riccio, A., and Clapham, D.E. (2011). Transient receptor potential cation channel, subfamily C, member 5 (TRPC5) is a cold-transducer in the peripheral nervous system. Proc. Natl. Acad. Sci. USA *108*, 18114–18119.